



1 **Inter-comparison of online and offline methods for measuring ambient heavy and trace elements**
2 **and water-soluble inorganic ions (NO_3^- , SO_4^{2-} , NH_4^+ and Cl^-) in $\text{PM}_{2.5}$ over a heavily polluted**
3 **megacity, Delhi**

4 Himadri Sekhar Bhowmik¹, Ashutosh Shukla¹, Vipul Lalchandani¹, Jay Dave³, Neeraj Rastogi³, Mayank
5 Kumar⁴, Vikram Singh⁵, and Sachchida Nand Tripathi²

6 ¹Department of Civil Engineering, Indian Institute of Technology Kanpur, Kanpur, India

7 ²Department of Civil Engineering and Centre for Environmental Science and Engineering, Indian Institute
8 of Technology Kanpur, Kanpur, India

9 ³Geosciences Division, Physical Research Laboratory, Ahmedabad, India

10 ⁴Department of Mechanical Engineering, Indian Institute of Technology Delhi, New Delhi, India

11 ⁵Department of Chemical Engineering, Indian Institute of Technology Delhi, New Delhi, India

12 *Correspondence to:* S. N. Tripathi (snt@iitk.ac.in)

13 **Keywords:** Aerosol mass spectrometer (AMS), Xact 625i ambient metal mass monitor, Ion
14 Chromatography (IC), ICP-MS, elemental composition.

15 **Abstract**

16 Characterizing the chemical composition of ambient particulate matter (PM) provides valuable information
17 on the concentration of secondary species, toxic metals and assists in the validation of abatement
18 techniques. The chemical components of PM can be measured by sampling on filters and analysing them
19 in the laboratory or using real-time measurements of the species. It is important for the accuracy of the PM
20 monitoring networks that measurements from the offline and online methods are comparable and biases are
21 known. The concentrations of water-soluble inorganic ions (NO_3^- , SO_4^{2-} , NH_4^+ and Cl^-) in $\text{PM}_{2.5}$ measured
22 from the 24 hrs filter samples using ion chromatography (IC) were compared with the online measurements
23 of inorganics from aerosol mass spectrometer (AMS) with a frequency of 2 mins. Also, the concentrations
24 of heavy and trace elements determined from the 24 hrs filter samples using inductively coupled plasma
25 mass spectroscopy (ICP-MS) were compared with the online measurements of half-hourly heavy and trace
26 metal's concentrations from Xact 625i ambient metal mass monitor. The comparison was performed over
27 two seasons (summer and winter) characterized by their different metrological conditions at IITD and
28 during winter at IITMD, two sites located in Delhi, NCR, India, one of the heavily polluted urban areas in



29 the world. Collocated deployments of the instruments helped to quantify the differences between online
30 and offline measurements and evaluate the possible reasons for positive and negative biases. The slopes for
31 SO_4^{2-} and NH_4^+ were closer to 1:1 line during winter and decreased during summer at both sites. The higher
32 concentrations on the filters were due to the formation of particulate $(\text{NH}_4)_2\text{SO}_4$. Filter-based NO_3^-
33 measurements were lower than online NO_3^- during summer at IITD and winter at IITMD due to the volatile
34 nature of NO_3^- from the filter substrate. Offline measured Cl^- was consistently higher than AMS derived Cl^-
35 during summer and winter at both sites. Based on their comparability characteristics, elements were
36 grouped under 3 categories. The online element data were highly correlated ($R^2 > 0.8$) with the offline
37 measurements for Al, K, Ca, Ti, Zn, Mn, Fe, Ba, and Pb during summer at IITD and winter at both the sites.
38 The higher correlation coefficient demonstrated the precision of the measurements of these
39 elements by both Xact 625i and ICP-MS. Some of these elements showed higher Xact 625i elemental
40 concentrations than ICP-MS measurements by an average of 10-40% depending on the season and site. The
41 reasons for the differences in the concentration of the elements could be the distance between two inlets for
42 the two methods, line interference between two elements in Xact measurements, sampling strategy, variable
43 concentrations of elements in blank filters and digestion protocol for ICP measurements.

44 **1. Introduction**

45 The adverse effect of ambient particulate matter (PM) on human health and the role of PM in visibility
46 degradation, altering earth's radiation balance, and climate change has received global attention in the last
47 two decades (Pope et al., 2009; Hong et al., 2019; Wang et al., 2019). To gain better insight into their
48 properties, the chemical characterization of particulate matter and its source attribution is crucial. The
49 National Capital Region (NCR), which includes India's capital (New Delhi) along with some districts
50 (Gurugram, Faridabad, and Noida) of the adjoining states of Haryana, Rajasthan, and Uttar Pradesh, is one
51 of the most polluted urban areas in northern India with a population over 47 million (Bhowmik et al., 2021).
52 According to World Economic Forum, New Delhi was listed as the most polluted city globally, with an
53 annual average $\text{PM}_{2.5}$ concentration of $\sim 140 \mu\text{g m}^{-3}$ (World Health Organisation, 2018). NCR has been a
54 specific area for researchers for the past couple of years due to its unprecedented $\text{PM}_{2.5}$ levels. Various large
55 and small scale industries, power plants, construction activities, and rapid increase in the vehicle numbers
56 (11 million in 2018) (Rai et al., 2020) are among the several causes that massively reduces the air quality
57 index (AQI) (Rai et al., 2020; Sharma & Kulshrestha, 2014). Further, the crop residue burning during the
58 month of Oct-Nov in the adjoining states of Haryana and Punjab on a larger scale worsens the air quality.

59 For decades, the mass concentrations of major water soluble inorganic ions (WSIS) and heavy and trace
60 metals in PM have been carried out by sampling them on filters and subsequently analysing them in



61 laboratory. Water-soluble inorganic ions (WSIS) and heavy and trace elements from these filter samples
62 are analyzed using ion chromatography (IC) (Bhowmik et al., 2021; Rengarajan et al., 2007; Rastogi &
63 Sarin, 2005) and inductively coupled plasma-mass spectroscopy (ICP-MS) or inductively coupled plasma-
64 optical emission spectroscopy (ICP-OES) (Patel et al., 2021) respectively. Usually, these filters are
65 collected over 24 hrs interval. Traditional receptor models usually use these offline measured data of very
66 low temporal resolution, making it challenging to characterize the short pollution episodes and dynamics
67 of pollution sources. Further, un-denuded filter sampling can have both negative and positive artifacts due
68 to volatile species (Lipfert, 1994; Pathak & Chan, 2005). The absorption of acidic and alkaline gases on the
69 filter substrates, if not removed prior to sampling, can give positive artifacts and result in overestimating
70 species concentration. Likewise, the evaporation of semi-volatile compounds (ammonium nitrate) from
71 filter substrates can give negative biases and result in underestimating aerosol concentration and its species
72 (Pathak & Chan, 2005; X. Zhang & McMurry, 1992). The degree of artifacts can be affected by several
73 factors, including temperature, relative humidity, type of filter substrate, the aerosol loading on the filter
74 substrate, etc. Transient events can also lead to mismatch. To overcome the limitations of low temporal
75 resolution and avoid the artifacts associated with offline filter sampling, methods have been developed for
76 measuring aerosol chemical composition at a higher time resolution in the order of hours or minutes.

77 Aerosol Mass Spectrometer (AMS) (Canagratna et al., 2007; Jayne et al., 2000; Jimenez et al., 2003) is one
78 kind of such instrument, which provides size-resolved chemical composition of non-refractory submicron
79 aerosols, e.g., organics, sulphate, nitrate, ammonium, and chloride at the order of hours or even minutes.
80 For other important components, such as calcium (main constituents of soil dust and construction activities)
81 and potassium (tracer of biomass burning), which AMS cannot measure, Xact ambient metal mass monitor
82 can be used. It is capable of measuring 40 elements, e.g., Al, Si, P, S, Cl, K, Ca, Ti, V, Cr, Mn, Fe, Co, Ni,
83 Cu, Zn, Ga, Ge, As, Se, Br, Rb, Sr, Y, Zr, Nb, Mo, Pd, Ag, Cd, In, Sn, Sb, Te, I, Cs, Ba, La, Ce, Pt, Au,
84 Hg, Tl, Pb and Bi with a frequency of every 30 mins to 4 hours. However, the high time-resolution
85 instruments measure lower range of species concentrations with higher limit of detection (LOD) than the
86 offline based methods (Tremper et al., 2018). Both offline and online methods have their own strength and
87 weaknesses. Uncertainties in offline filter analysis methods have been extensively studied (Pathak & Chan,
88 2005; Viana et al., 2006), but the novel online methods pose new problems (Wu & Wang, 2007). For
89 example, when the ambient concentrations are very low, online measurements are often close to the MDL
90 values due to the short integration times (Malaguti et al., 2015).

91 Previous studies in Delhi-NCR have used low time resolution filter-based methods for chemical
92 characterization of submicron aerosols (Bhowmik et al., 2020; Nagar et al., 2017; Pant et al., 2015; S. K.
93 Sharma et al., 2016; Singhai et al., 2017). On the other hand, there are only a few studies in Delhi-NCR



94 that used high time resolution methods (HR-ToF-AMS, Q-ACSM, Xact) for characterization and source
95 apportionment of coarse and fine particulate matters (Gani et al., 2019; Lalchandani et al., 2021; Rai et al.,
96 2020, 2021; Singh et al., 2021; Tobler et al., 2020). Online and offline measurements both have their
97 advantages and limitations. For both these measurements, the quality of the data highly depends on the
98 calibration of the instruments. For Xact, the multi-element mix standard might not represent ambient
99 elemental mix if the ambient particulate matters are too low or too high in concentration, affecting the
100 collection properties of the filter (Indresand et al., 2013). For filter-based water-soluble inorganic ion and
101 metal analysis, confidence in the data depends on the calibration as well as the volatility, solubility, and
102 digestion protocol used for the extraction of water-soluble inorganic ions and elements, respectively. Thus,
103 it is vital for monitoring networks that both the offline and online measurement methods give comparable
104 results. Few published studies have compared inorganics and elements from filter-based measurements and
105 semi-continuous methods (e.g., Furger et al., 2017; Nie et al., 2010). The inter-comparison in these studies
106 is unjustified for highly polluted areas, as the specie values observed in these studies are much below MDL
107 due to very low ambient concentration of secondary species and elements. It will be interesting to study the
108 inter-comparison in highly polluted areas. To the best of our knowledge, there are neither any published
109 seasonal and temporal comparisons of inorganics from high time resolution AMS measurements and filter-
110 based measurements from ion chromatography nor any comparisons of heavy and trace metals from high
111 time resolution Xact 625 ambient metal mass monitor and offline measurements from ICP-MS in the
112 heavily polluted Delhi NCR region.

113 This study demonstrates a comparison between online and offline measurements of WSIS and heavy and
114 trace metals at two sites in Delhi NCR during summer (June-July 2019), characterized by moderate levels
115 of local pollution and winter (October-December 2019), affected by high levels of pollution from local
116 sources and regional transport of crop residue burning emissions from adjoining state of Haryana and
117 Punjab.

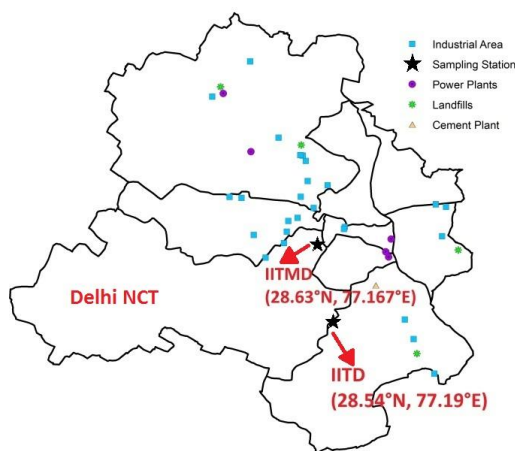
118 **2. Methodology**

119 **2.1. Sampling sites**

120 Delhi-NCR, a highly polluted urban area with an annual average $PM_{2.5}$ concentration of $140 \mu g m^{-3}$ and a
121 population of over 47 million, is surrounded by the Thar desert on its west and Indo-Gangetic Plain on its
122 east to south-east. The temperature is about $\sim 35^{\circ}C$ - $48^{\circ}C$ during summer (April-June), and winter
123 (December-February) is relatively cooler, with temperature ranges from $\sim 2^{\circ}C$ - $15^{\circ}C$ (Bhowmik et al., 2020;



124 Lalchandani et al., 2021; Tobler et al., 2020). The wind is mostly north-westerly during both summer and
125 winter.



126

127 Fig.1. Sampling sites with various emission sources like power plants, industries, landfills, etc.

128 2.1.1. Delhi NCR site 1: IITD

129 High volume PM_{2.5} samples were collected on the rooftop of the Centre for Atmospheric Science (CAS)
130 building at the Indian Institute of Technology, Delhi (IITD) (28.54°N, 77.19°E; ~218 m amsl) about ~15
131 m above the ground level. Further, one HR-ToF-AMS and Xact ambient metal mass monitor were deployed
132 inside a temperature-controlled laboratory on the 3rd floor of the same building about ~10 m above the
133 ground level. It is an educational institute cum residential campus having restaurants nearby and very close
134 to (<200 m) heavy traffic road. Lalchandani et al., (2021); Rai et al., (2020) observed source signatures of
135 emissions from industries, power plants, vehicles, and waste burning in this site.

136 2.1.2. Delhi NCR site 2: IITMD.

137 Offline PM_{2.5} sampling was carried out on the rooftop of the main building at the Indian Institute of Tropical
138 Meteorology Delhi (IITMD) (28.63°N, 77.167°E; ~220 m above msl) about 15 m above the ground level.
139 Moreover, HR-ToF-AMS and Xact ambient metal mass monitor were installed inside a temperature-
140 controlled laboratory on the 2nd floor of the same building at the height of ~8 m from the ground level. This
141 site is placed in the central urban area of Delhi and surrounded by Central Ridge reserve forest and
142 residential areas (Tobler et al., 2020) and around 14 km away in North West direction from IITD. A recent



143 study by Lalchandani et al. (2021) observed the site is dominated by emissions from traffic, solid fuel
144 burning, and oxidized organic aerosols. The location of the sampling sites are shown in Fig. 1.

145 **2.2. Sampling details**

146 **2.2.1 Offline sampling**

147 Biweekly 24 hrs (January- September 2019) and daily 24 h (October- December 2019) PM_{2.5} samples were
148 collected on quartz filter substrates (Whatman; 8 × 12 inches) using a high-volume sampler (HVS) with a
149 flow rate of 1.13 m³/min. Blanks were collected in the field by placing a fresh filter in the sampler while
150 not running. The collected filters, including field blanks, were zip-locked and stored in the freezer at each
151 site and periodically transported to CESE (Centre for Environmental Science and Engineering), IIT Kanpur,
152 where they were further stored at -20°C in a deep freezer prior to analysis. For this study, the samples from
153 the common period of offline and online sampling (October-December 2019) from the two sites were
154 analyzed for WSIS (SO₄²⁻, NO₃⁻, NH₄⁺ and Cl⁻) using an IC, and 32 metals (Al, Na, K, Ca, Ti, V, Cr, Mn,
155 Fe, Ni, Cu, Zn, As, Se, Rb, Sr, Zr, Cd, Sn, Sb, Ba, Pb, Cs, La, Ce, Pt, Tl, Mg, Li, Mo, Co and Pd) using an
156 ICP-MS. More details of analytical procedures are given in the instrumentation section.

157 **2.2.2 Online sampling**

158 At both IITD and IITMD site, high-resolution time-of-flight aerosol mass spectrometers (HR-ToF-AMS,
159 Aerodyne Research Inc., Billerica, MA) (Canagaratna et al., 2007; DeCarlo et al., 2006), equipped with
160 PM_{2.5} aerodynamic lens (Peck et al., 2016) (Aerodyne Research Inc., Billerica, MA, USA) were installed.
161 Ambient fine particulate matters were sampled through PM_{2.5} cyclone (BGI, Mesa Labs. Inc.) inlet at IITD
162 and through black silicon tubing at IITMD, placed ~1.5-2 m above the rooftop with a flow rate of 5 l/min
163 using long stainless-steel tubing (12 mm O.D). An aerosol sample dryer system (Aerodyne research, Inc)
164 was used to dry the ambient aerosols to maintain the output RH at 20%. At IITD, data were collected from
165 12th October 2019-31st December 2019 and 2nd June 2019-21st July 2019 during winter and summer
166 campaigns respectively. The data between 1st November and 14th November was not available, due to
167 hardware issues in the AMS during that period. At IITMD, data were only collected during winter campaign
168 from 25th October 2019 to 31st December 2019.

169 Two Xact 625i ambient metal monitors (Cooper Environmental Services, Beaverton, Oregon, USA) were
170 installed at IITD and IITMD. Ambient aerosols were sampled through a PM_{2.5} inlet with a flow rate of 16.7
171 lpm. At IITD, sampling was carried out from 1st October 2019-31st December 2019 and 30th May 2019-25th
172 July 2019 during the winter and summer campaign, respectively. However, data between 16th July and 24th



173 July were not available due to hardware breakdown. At IITMD, samples were collected from 1st October
174 2019-31st December 2019 but data from 18th November to 26th November 2019 and 30th November to 14th
175 December 2019 were not available due to instrumental problems.

176 Online measurements of inorganic ions (SO₄²⁻, NO₃⁻, NH₄⁺ and Cl⁻) from HR-ToF-AMS were compared
177 with the WSIS using an IC. Parallely, heavy and trace metals obtained from Xact ambient metal mass
178 monitor were compared with the metal data from the offline filter measurements using an ICP-MS. Though
179 the sampling periods of AMS, Xact, and HVS were different for different seasons and different sites as well
180 (Table 1), only the common periods of online and offline sampling have been discussed in this study for
181 comparison.

182 Table 1. Sampling strategy and instrumentation used.

	Interval	IITD	IITMD
Quartz filter Sampling	3 days	January-September 2019	January-September 2019
	24 hrs	October-December 2019	October-December 2019
HR-ToF-AMS	2 mins	2 nd June-21 st July 2019	25 th October-31 st December 2019
		12 nd October-31 st December 2019	
Xact	30 mins	30 th May-25 th July 2019	1 st October-31 st December 2019
		1 st October-31 st December 2019	

183 Filters from the common periods were analysed for WSIS and heavy and trace metals using an IC and ICP-MS respectively.

184 2.3. Instrument details

185 2.3.1 WSIS measurements by IC and HR-ToF-AMS

186 For WSIS analysis, 9 sq.cm punch area of each collected filter was soaked in 30 ml of high purity milli-q
187 water (resistivity-18.20 MΩ cm) for 12 hours in pre-cleaned borosilicate test tubes to ensure maximum
188 solubility. The amount of water added, soaking time, etc. effect the solubility of the ions as well as the
189 extent of extraction. Details can be found in our previous paper (Bhowmik et al., 2020). Soaked samples
190 were filtered through 0.22 μm quartz filter papers to remove any suspended contaminations after an
191 ultrasonication for 50 mins. Cl⁻, NO₃⁻, SO₄²⁻ and, NH₄⁺ were measured for all the filter extracts by an IC
192 (Metrohm 883 Basic IC plus for cations and 882 compact IC plus for anions). Separate columns for the
193 analysis of cations and anions were installed in two separate modules. For anion and cation separation, an



194 AS 5-250/4.0 chromatography column and C-6 column was used, respectively. The sample carried by 3.2
195 mM Na₂CO₃+1 mM NaHCO₃ solution and 2.7 mM HNO₃ solution in the anion and cation module
196 separately passes through the charged columns to analyze each ion according to their polarity. The
197 calibration was performed by a seven-point method with a range of standards prepared by the serial dilution
198 from the stock solution standard of 10 ppm purchased from Metrohm. The uncertainty of the water-soluble
199 inorganic ions measured by IC was estimated as 4% (coverage factor~2) by the approach described in
200 Yardley et al. (2007).

201 HR-ToF-AMS measures size-resolved mass spectra of non-refractory particles (PM components that
202 vaporize at 600°C and 10⁻⁵ Torr, e.g., organics, nitrate, sulphate, ammonium, and some chlorides) of
203 submicron particulate matters. The details of this instrument can be found elsewhere (DeCarlo et al., 2006).
204 Briefly, ambient aerosols are collected through an orifice of 100 µm diameter and focused into a narrow
205 particle beam by an aerodynamic lens system installed inside the instrument, which has a transmission
206 efficiency of > 50% for PM_{2.5} (DeCarlo et al., 2006; Peck et al., 2016). The particle size is determined after
207 analyzing the time of flight, i.e., time taken to travel along the length of the sizing chamber. The NR-PMs
208 are then vaporized by hitting the vaporizer at 600°C and at a vacuum of 10⁻⁷ Torr. Further, the vaporized
209 molecules are electronically ionized at 70 eV, followed by detection by a mass spectrometer as per their
210 *m/z*. HR-ToF-AMS can be operated in W-mode or V-mode. For this study, it was operated in V-mode with
211 a sampling time of 2 mins. Mass spectra (MS) mode, in which mass spectra of the components are
212 measured, and particle time-of-flight (PToF) mode in which the size-resolved mass spectra are measured,
213 are alternated in every 30s in 2 cycles. The HR-ToF-AMS was calibrated using standard protocols provided
214 in our previous publication (Lalchandani et al., 2021; Singh et al., 2019).

215 To determine the mass concentration of NR-PMs, Unit mass resolution (UMR) analysis was done using the
216 SQUIRREL data analysis toolkit (version 1.59) programmed in IGOR Pro 6.37 software (Wavemetrics,
217 Inc., Portland, OR, USA). High resolution (HR) analysis was also done on the data set using Peak Integrated
218 Key Analysis (PIKA version 1.19) toolkit. At the beginning of each campaign at the two sites, ionization
219 efficiency calibration was performed by injecting mono-disperse 300 nm ammonium nitrate and ammonium
220 sulphate particles into AMS and a condensation particle counter (Jayne et al., 2000). More details can be
221 found in Lalchandani et al. (2021) (manuscript under review).

222 **2.3.2 Heavy and trace metal measurements by ICP-MS and Xact 625i**

223 For the analysis of heavy and trace metals, 15 sq. cm area of each collected filter was digested in an acid
224 mix of 0.5 ml HF+1.5 ml HNO₃ for 4 hours within closed HDPE Teflon tubes using a Hot plate (Savillex-



225 HF resistive Model number 88888:00000). The temperature range should be ~90-120°C to ensure complete
226 digestion of the elements. Further, 2.5 ml of HClO₄ was added to the precipitates, left over the Teflon tube
227 wall and the tubes were kept on the hot plate at 220-240°C for another 4 hours with the lids open for
228 complete evaporation of the acid mix. Moreover, the residual was dissolved in 6N HNO₃ and diluted with
229 de-ionized water (resistivity-18.20 MΩ cm) followed by filtering through 0.22 μm quartz filter papers prior
230 analysis. Details can be found in our forthcoming paper. This method is well established and used in many
231 studies (Minguillón et al., 2012; Querol et al., 2008).

232 Thirty two metals (Al, Na, K, Ca, Ti, V, Cr, Mn, Fe, Ni, Cu, Zn, As, Se, Rb, Sr, Zr, Cd, Sn, Sb, Ba, Pb, Cs,
233 La, Ce, Pt, Tl, Mg, Li, Mo, Co and Pd) were analyzed for all filter extracts using an ICP-MS (Thermo
234 Scientific iCAP Q ICP-MS) at IIT Kanpur Environmental Engineering laboratory. Si could not be
235 determined in the filter samples because Si is the primary constituent of the quartz filters and hence digested
236 during sample preparation. Samples were first introduced to a nebulizer using an injector attached to an
237 autosampler for transformation into fine aerosol droplets followed by ionization at a very high temperature
238 (8000K) in Ar-plasma. The elements elute as per their *m/z*. A known concentration (5 ppb) of Ge was used
239 as an internal standard to monitor the instrumental drift during the analysis. The overall average drift was
240 reported as ± 10%. The calibration was performed by ten-point method with a range of mix standards
241 prepared by the serial dilution from the High purity multi-element (35 elements) standards (soluble in 1%
242 HNO₃, 100 ppm) purchased from Sigma Aldrich.

243 The Xact 625i Ambient Metals Monitor (Cooper Environmental Services (CES), Beaverton, OR, USA)
244 uses X-ray fluorescence to measure the real-time elemental data in particulate matter. For this study, a PM_{2.5}
245 inlet was used. Details of the instrument can be found in Furger et al., 2017. Briefly, aerosol samples were
246 collected on a Teflon filter tape followed by hitting the loaded area with X-rays and the fluorescence
247 measured by a silicon drift detector (SDD). Thirty elements: Al, Si, S, Cl, K, Ca, Ti, Cr, Mn, Fe, Co, Ni,
248 Cu, Zn, As, Se, Br, Rb, Sr, Zr, Mo, Cd, In, Sn, Sb, Te, Ba, Pb, Bi, and Bi were measured with 30 min time
249 resolution. The Xact 625i was calibrated during each campaign using thin film standards for the individual
250 elements. The reproducibility was observed within ± 5%. Every midnight energy alignment checks were
251 performed for 15 mins (00:15 to 00:30) (for Cr, Pb, Cd and Nb). An uncertainty of ~10% was reported by
252 the manufacturer in an interference free situation (USEPA & Etv, 2012). This included 1.73% from flow
253 (CEN, 2014), 5% for standard reproducibility or uncertainty during calibration (USEPA, 1999) and 2.9%
254 from term stability as reported in Tremper et al. (2018). More details on the instrumental set up and stability
255 check during the summer and winter campaign can be found in Rai et al. (2020) and Shukla et al. (2021).

256 3. Results and discussions



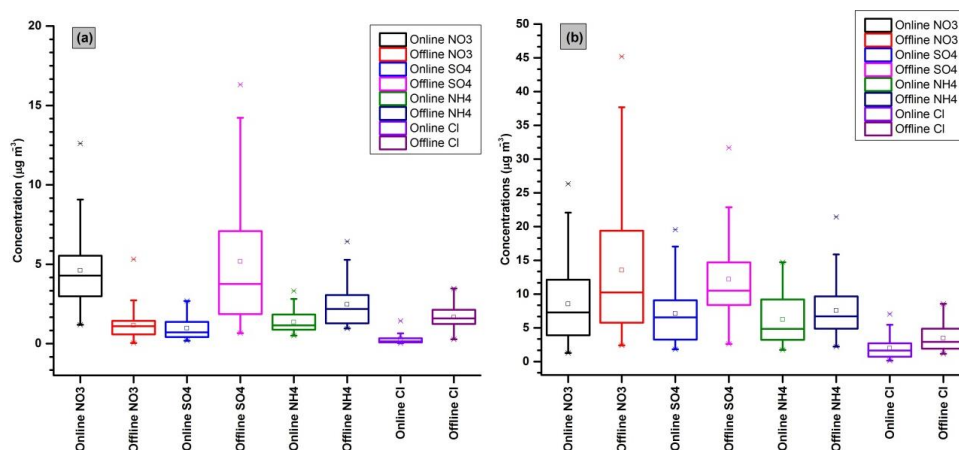
257 3.1. Online and offline measurements of WSIS and their comparison

258 Large temporal variability was observed in both offline and online measurements of WSIS (NO_3^- , SO_4^{2-}
259 and, NH_4^+ and Cl^-) during the winter campaign and summer campaign at both sites. The inorganics data
260 with 2 mins interval from HR-ToF-AMS were averaged over the sampling period of the filters, i.e., 24
261 hours. The time series of NO_3^- , SO_4^{2-} , NH_4^+ , and Cl^- during the summer and winter campaign at IITD and
262 winter campaign at IITMD are shown in Fig. SM1 in the supplementary material. Higher peaks of
263 inorganics were observed during 25th Oct-18th Nov during the winter campaign at IITD, which was the
264 agricultural crop-residue burning period (Nagar et al., 2017). During the winter campaign, NO_3^- was the
265 most abundant ion followed by SO_4^{2-} , NH_4^+ and Cl^- for both offline and online measurements at both the
266 sites whereas, during the summer campaign at IITD, NO_3^- was the most abundant ion followed by NH_4^+ ,
267 SO_4^{2-} and Cl^- in online measurement (HR-ToF-AMS). Similar results were observed in our companion
268 paper, Shukla et al. (2021). Interestingly, in the case of offline measurements during the summer campaign
269 at IITD, NO_3^- was least abundant, and the sequence changed as $\text{SO}_4^{2-} > \text{NH}_4^+ > \text{Cl}^- > \text{NO}_3^-$. The average
270 concentrations with their ranges are tabulated in Table SM1 in supplementary material, and the mean,
271 maximum and minimum concentration are shown in Fig. 2 using box plots.

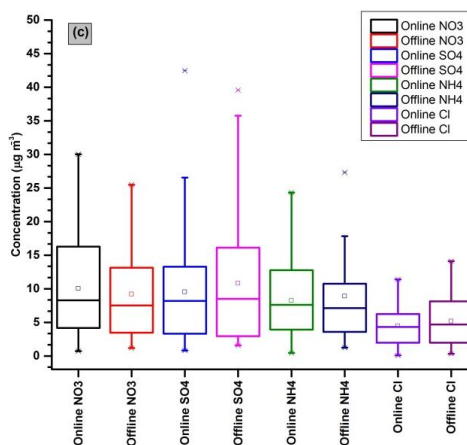
272 Comparability and correlation between offline and online measurements were evaluated in this study by
273 applying linear regression using offline data as the independent and online data as the dependent variable.
274 The comparability of NH_4^+ measurements was observed to be good for both summer and winter campaigns
275 at both sites. During the winter campaign, the correlations were $R^2=0.76$, and $R^2=0.89$, and the slopes were
276 closer to 1 (0.99 for IITD and 0.93 for IITMD) for IITD and IITMD, respectively (Fig. 3). Interestingly
277 during the summer campaign at IITD, though the correlation improves ($R^2=0.91$), the slope decreases to
278 0.49. This is because the vapor concentration of sulfuric acid (H_2SO_4) is negligible during winters and
279 higher during summers. As a result of which, the adsorption of sulfuric acid on PM deposited on the filter
280 papers happens during summers which react with gaseous ammonia (NH_3) to form particulate $(\text{NH}_4)_2\text{SO}_4$
281 (D. Zhang et al., 2000), thus increasing ammonium concentration in the offline measurements during the
282 warmer season, especially in the presence of dust (Nicolás et al., 2009).



283



284



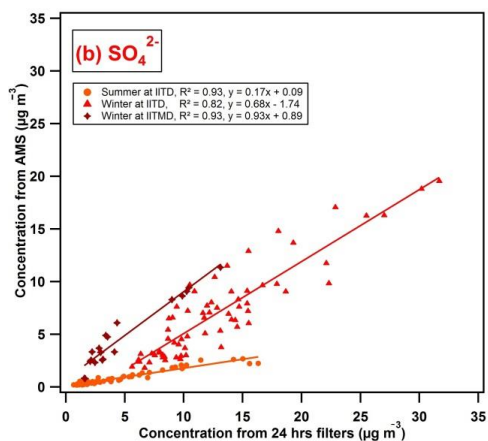
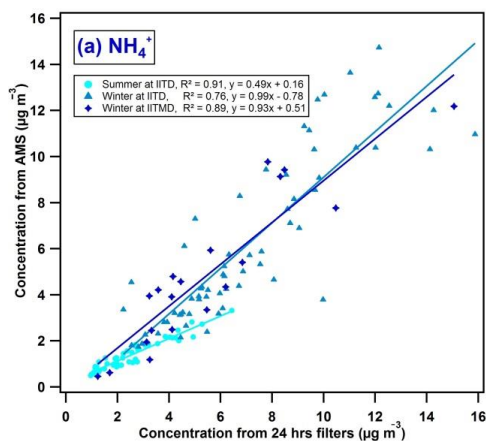
285 Fig.2. Box plots of online and offline measured secondary species (NO_3^- , SO_4^{2-} and, NH_4^+) and Cl⁻ during
286 (a) summer campaign at IITD, (b) winter campaign at IITD, and (c) winter campaign at IITMD site.

287 The filter-based measurements of SO_4^{2-} were higher than those from the online measurements for IITD and
288 IITMD during both the seasons (Fig. 2). Their comparability is characterized by a correlation coefficient of
289 $R^2=0.93$ with a slope of 0.17 and $R^2=0.82$ with a slope of 0.68 at IITD during the summer and winter
290 campaigns, respectively. Interestingly, offline SO_4^{2-} data correlates well with online SO_4^{2-} data having a
291 correlation coefficient of $R^2=0.93$ with a slope close to 1 (0.93) during the winter campaign at IITMD (Fig.
292 3). A slope of less than 0.5 was observed in Malaguti et al., (2015) in Italy during the warm period whereas
293 the offline measurement of SO_4^{2-} was 34% lesser than the AMS measurements in Pandolfi et al., (2014).
294 The higher SO_4^{2-} concentrations on the un-denuded offline filter-based measurements were possibly
295 because of the positive sampling artifact. SO_2 is absorbed in the filter by the collected alkaline particles

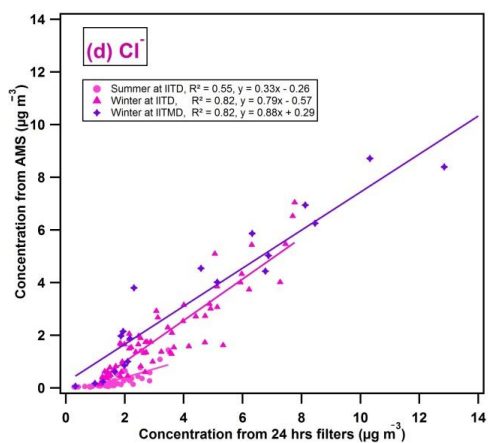
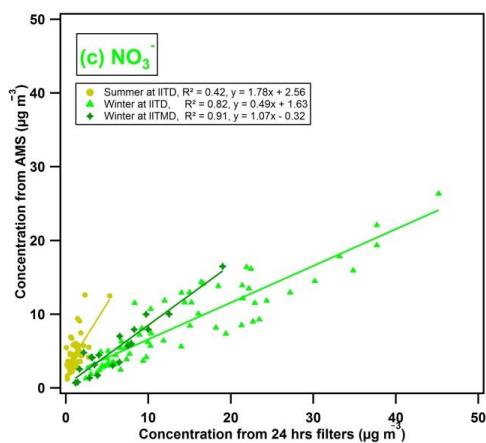


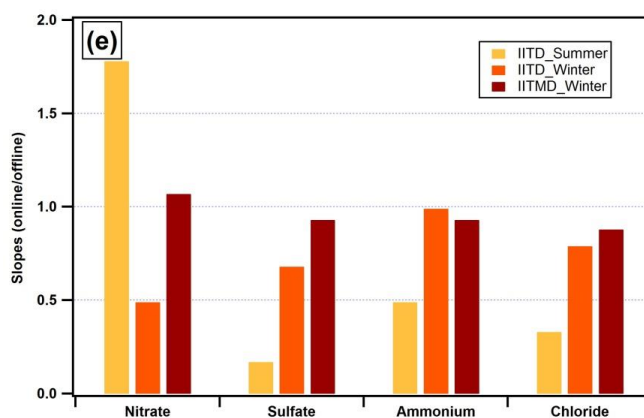
296 (Nie et al., 2010). The higher concentration could also be due to the formation of particulate $(\text{NH}_4)_2\text{SO}_4$
297 because of the earlier discussed reactions between gas-phase NH_3 and H_2SO_4 formed on the fine particles
298 (Nicolás et al., 2009).

299



300





301

302 Fig.3. Scatter plots between online and offline measured (a) NH_4^+ , (b) SO_4^{2-} , (c) NO_3^- , (d) Cl^- concentrations
303 and (e) comparison of slopes (online/offline) of the measured inorganic ions in $\text{PM}_{2.5}$ during summer and
304 winter campaign at IITD and during winter campaign at IITMD.

305 The NO_3^- concentrations measured by the HR-ToF-AMS were higher than the offline data during summer
306 at IITD and during winter at IITMD whereas, filter-based measurements of NO_3^- were higher during winter
307 at IITD (Fig. 2). The online and offline measurements posed a good correlation during winter ($R^2 = 0.91$
308 and slope of 1.07 at IITMD, $R^2 = 0.82$ and slope of 0.49 at IITD). The linearity worsens during summer at
309 IITD ($R^2 = 0.42$ and slope of 1.78) (Fig. 3). The slopes and correlation coefficient for the WSIS are listed
310 in Table 2. Pandolfi et al., (2014) observed NO_3^- HR-AMS/Filter ratios of ~ 1.7 at Barcelona and Montseny
311 in Europe. The higher offline NO_3^- concentrations during winter at IITD can be possibly because of the
312 positive artifact due to the absorption of gas-phase nitric acid (HNO_3) on the filter (Chow, 1995). Many
313 studies (Chow et al., 2008; Kuokka et al., 2007; Malaguti et al., 2015) reported higher concentrations of
314 NO_3^- from high time resolution measurements than filter-based measurements due to the evaporation of
315 ammonium nitrate collected on filters over the duration of sample collection (Pakkanen & Hillamo, 2002;
316 Schaap et al., 2004; Kuokka et al., 2007). This evaporation loss increases with the decrease of humidity and
317 the increase of temperature (Chow et al., 2008; Takahama et al., 2004). Also, complete evaporation may
318 occur beyond 25°C (Schaap et al., 2004). The high temperature (35°C - 48°C) during the long sampling
319 hours (24 hours) may be a possible reason for the poor correlation between online and offline NO_3^-
320 measurements during the summer campaign at IITD. Chow et al., (2008) observed the evaporation loss
321 from quartz filter to be more than 80% during the warm season in central California. A study by Schaap et
322 al., (2004) reported that the NO_3^- volatilization during a 24-h sampling period not only depends on the
323 sampling apparatus and ambient conditions, but also a function of sampling strategy. If the sampling



324 strategy is evening to evening (24 hours), the samples will lose the NO_3^- during night as evaporation
325 increases during the day with the increase in temperature. However, during morning-to-morning strategy,
326 the filters will collect the NO_3^- at night, and the higher temperature in the afternoon of the previous day
327 may promote the loss of NO_3^- from the filter (Malaguti et al., 2015). In this study, the sampling time was
328 from 6:30 am to the next day 6.30 am. Therefore, the filter-based inorganic measurements suffered from a
329 negative sampling artifact due to the evaporation of nitrate collected during the forenoon in a temperature
330 of 20°C - 25°C during the winter campaign and $\sim 38^\circ\text{C}$ - 45°C during the summer campaign.

331 Table 2. Regression coefficients and slopes for the comparison of WSIS measured by HR-ToF-AMS and
332 IC.

Sites	NO_3^-		SO_4^{2-}		NH_4^+		Cl^-	
	R^2	Slope	R^2	Slope	R^2	Slope	R^2	Slope
IITD Summer	0.42	1.78	0.93	0.17	0.91	0.49	0.55	0.33
IITD Winter	0.82	0.49	0.82	0.68	0.76	0.99	0.82	0.79
IITMD Winter	0.91	1.07	0.93	0.93	0.89	0.93	0.82	0.88

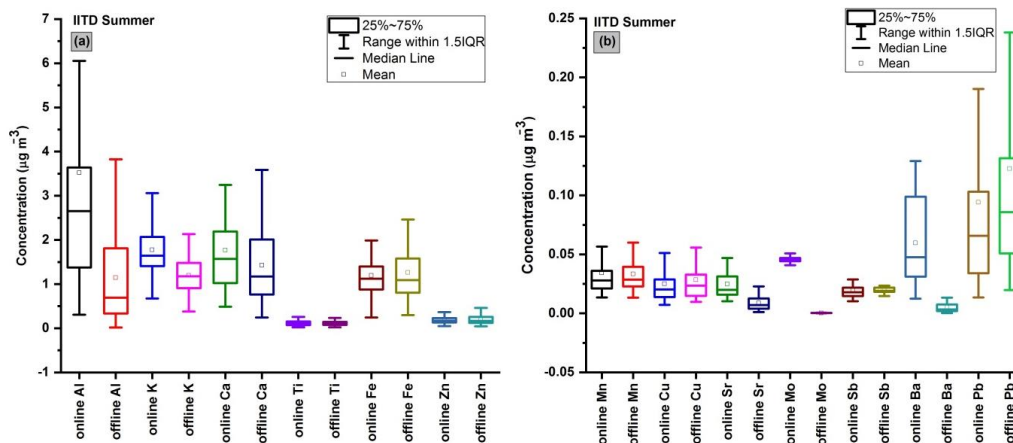
333 We observed higher Cl^- concentration in filter-based measurement than online measurement using HR-ToF-
334 AMS during both campaigns at IITD and winter at IITMD. A good correlation of $R^2=0.82$ with a slope of
335 0.79 and $R^2=0.82$ with a slope of 0.88 was observed during the winter campaign at IITD and IITMD,
336 respectively (Fig. 3). Interestingly, during the summer campaign at IITD the comparability was moderate
337 with a correlation coefficient of $R^2=0.55$ and a slope of 0.33 . A correlation coefficient of $R^2=0.83$ between
338 $\text{Dp} < 10 \mu\text{m}$ measured with the MARGA and analyzed from Teflon filters was reported in Makkonen et al.,
339 (2012) during Feb-May. We also compared Cl^- measurements from Xact 625i with the measurements from
340 IC. IC measurements of Cl^- were also found to be higher than Xact 625i measurements during summer at
341 IITD and winter at IITMD. Interestingly, the Cl^- measurements from Xact 625i were ~ 1.9 times higher than
342 the measurements from IC during winter at IITD (see fig. SM2 in supplementary material). The correlations
343 were found to be good during winter ($R^2=0.83$ and 0.76 at IITD and IITMD respectively) and worsen
344 during summer ($R^2=0.27$ at IITD), similar to what we observed for AMS_Cl^- and IC_Cl^- . Lower
345 temperature and higher RH during winter retains Cl^- in particulate phase for long enough to be detected
346 which is not the case in summer. Further, Cl^- is predominantly found in the coarse fraction. Also, while
347 AMS only measures the NR- Cl^- (Manchanda et al., 2021), e.g. NH_4Cl , which can vaporize at 600°C but
348 cannot measure Cl^- from refractory-KCl, IC measures chloride from all the water-soluble chloride salts,
349 including NH_4Cl and KCl. On the other hand, Xact 625i measures Cl^- from both the salts using XRF
350 technique. This probably justifies the lower concentration of Cl^- in online measurements than filter-based
351 measurements and better slopes (closer to unity) with Xact than AMS.



352 3.2 Online and offline measurements of heavy and trace metals and their comparison

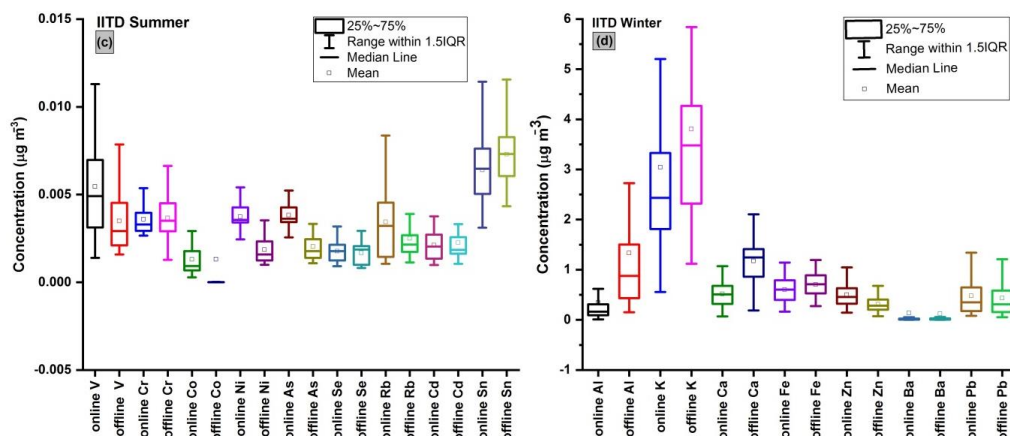
353 For the inter-comparison of heavy and trace metal concentrations from Xact 625i and ICP-MS, the half-
354 hourly Xact 625i data were averaged to 24 hours filter sampling interval. A total of 32 elements were
355 analyzed on each filter using ICP-MS while, 27 elements were measured in Xact 625i at IITD during
356 summer and winter campaign, and 30 elements were measured in Xact 625i at IITMD during the winter
357 campaign. The spatial and temporal variations of the crustal and trace elements are shown in Fig. SM3. Al
358 and Ca concentrations were the most abundant in ICP-MS and Xact measurements respectively during the
359 summer season (Fig. 4a, 5a & 5b) because of the increase in the crustal activities whereas K concentrations
360 were significantly high for both the measurements during winter (Fig. 4d, 4g, 5c, 5d, 5e and 5f) due to
361 mass-scale agricultural crop-residue burning in the adjoining states of Punjab and Haryana. Elements
362 emitted from anthropogenic activities, e.g., coal-fired power plants (As, Se, Hg, Pb), traffic emissions (Cr,
363 Pb, Mn), wear debris emission (Cu, Cd, Fe, Ga, Mn, Mo), etc. are found to be in higher concentration during
364 winter campaign than summer campaign for both the measurements. Similar results were observed in our
365 companion paper Shukla et al. (2021). The average values of metals along with their ranges are tabulated
366 in Table SM2 and the statistics involved mean, upper, and lower values are shown in Fig. 4.

367

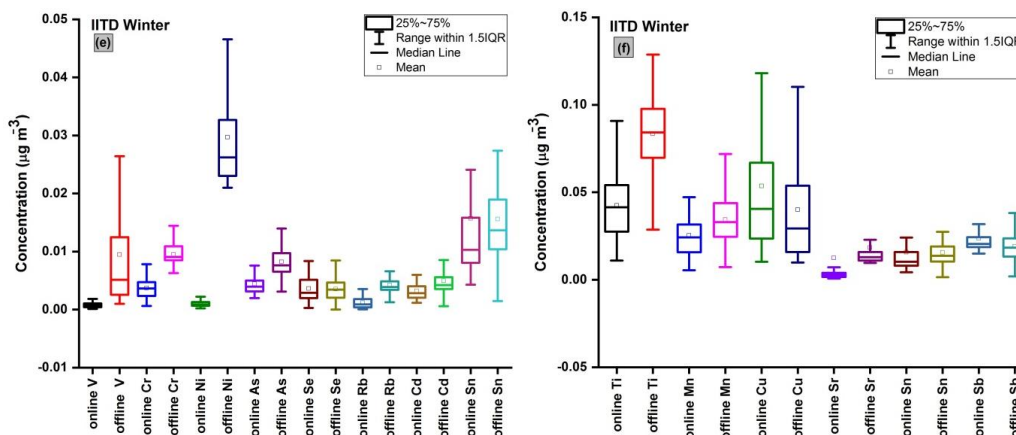




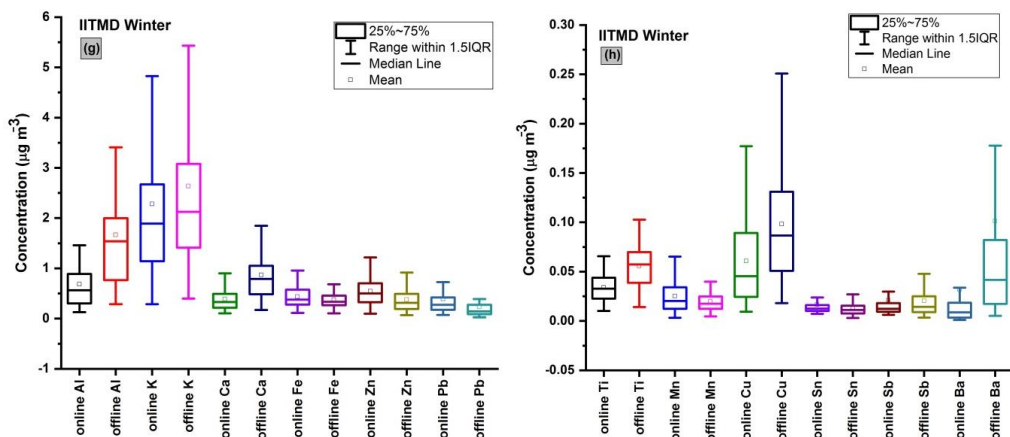
368

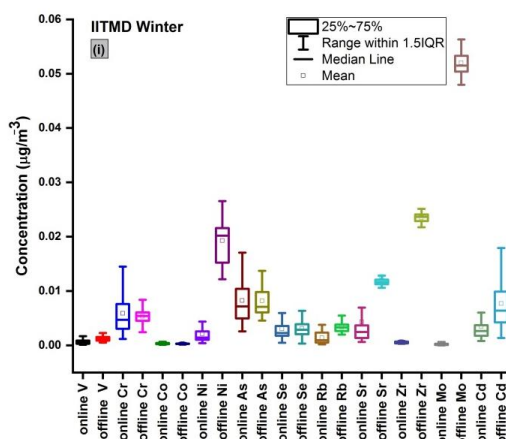


369



370



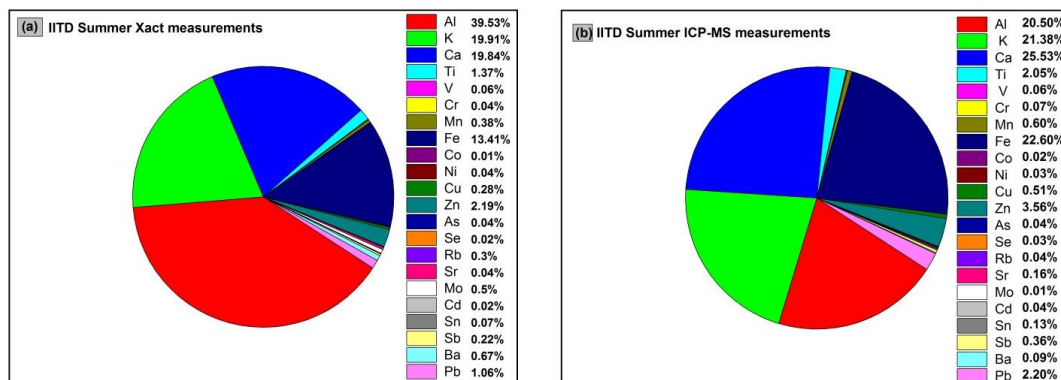


371

372 Fig.4. Box plots of online and offline measured heavy and trace metals during (a,b,c) summer campaign at
 373 IITD, (d,e,f) winter campaign at IITD, and (g,h,i) winter campaign at IITMD site.

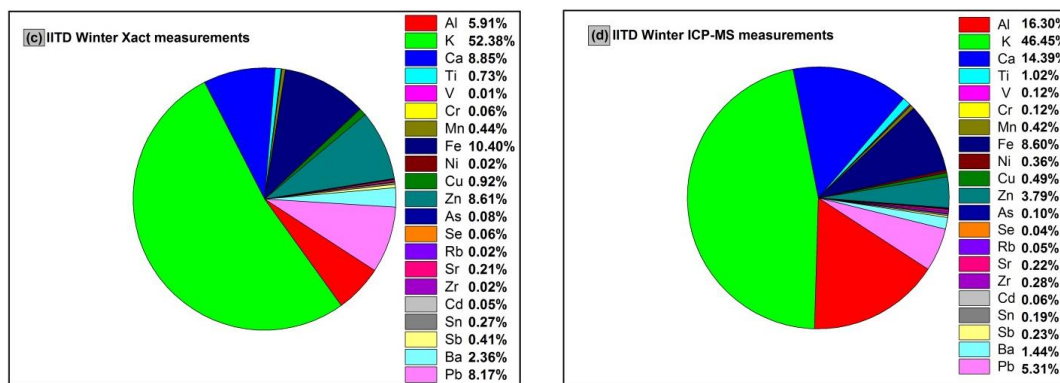
374 The trends of the elemental concentration in decreasing order for both ICP-MS and Xact measurements
 375 during summer and winter at IITD and winter at IITMD are shown in Fig. SM4. The trace metals such as
 376 Cd, Mn, Mo, Ba, Pd etc. contribute a small portion in $\text{PM}_{2.5}$ in terms of their mass concentration but have a
 377 significant effect on human health. Fractions of elements in total element concentration for both the
 378 measurements during summer and winter campaign at IITD and during winter campaign at IITMD were
 379 shown in Fig. 5.

380

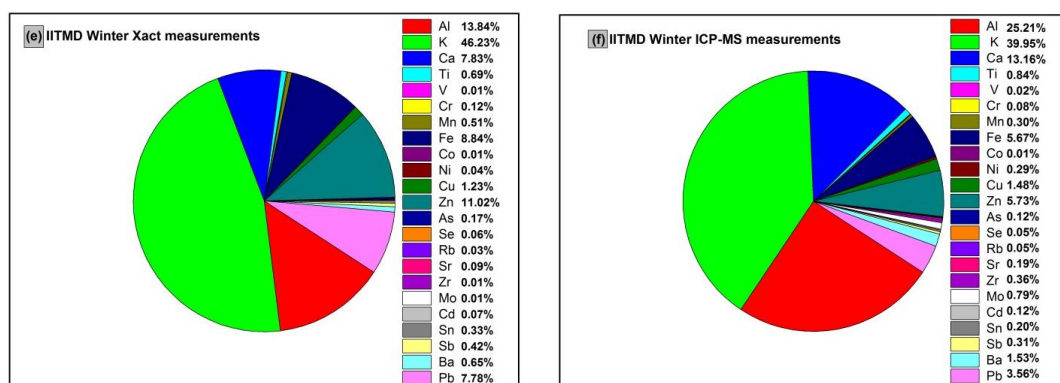




381



382

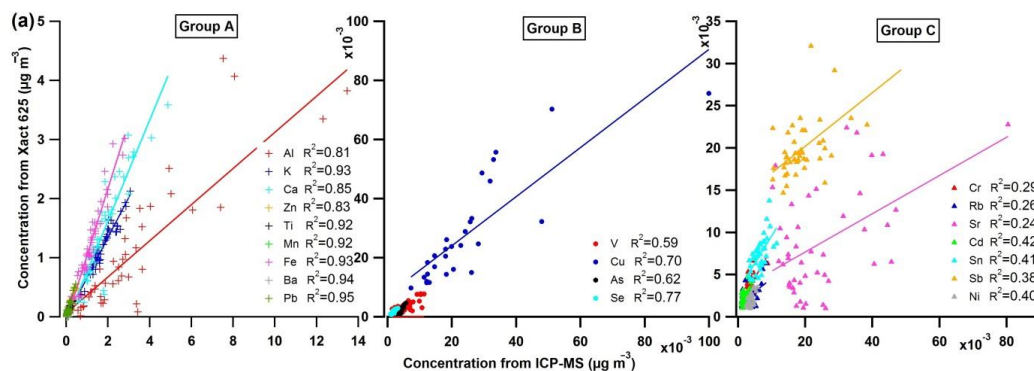


383 Fig.5. Fractions (%) of elements in total element concentration in PM_{2.5} presented in pie format for online
 384 (a,c,e) and offline (b,d,f) measurements during winter and summer at IITD and during winter at IITMD.

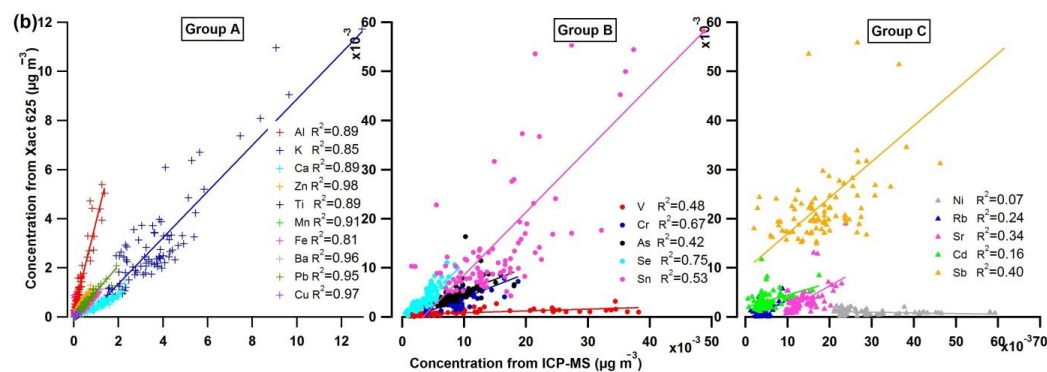
385 MDLs for ICP-MS measurements were calculated according to Escrig Vidal et al., (2009), and MDLs for
 386 Xact 625i were obtained from the manufacturer. MDLs for the Xact 625i and ICP-MS are listed in Table
 387 SM2 in the supplementary material. Though the half-hourly Xact data were averaged to 24 hours to the
 388 corresponding interval of the filter sampling, for comparability check, MDLs of Xact 625i measurements
 389 were taken for 30 mins sampling time while MDLs of filter-based elemental measurements were calculated
 390 for 24 hours. Data below $3 \times$ MDL value were discarded from the data set as it would lead to higher
 391 uncertainty (Furger et al., 2017). The elements K, Ca, Ti, Mn, Fe, Ba, and Pb have >80% of their values
 392 above both offline and online MDLs, and thus the data quality is reliable. Further, Ni, Mo, Zr have higher
 393 blank concentrations, and thus the data is not reliable for ICP-MS measurements. The comparability of the
 394 elements measured online using Xact 625i with those analysed using an ICP-MS, was checked for the
 395 common elements in these two measurements (21 elements for IITD and 23 elements for IITMD) and is
 396 shown in Fig. 6.



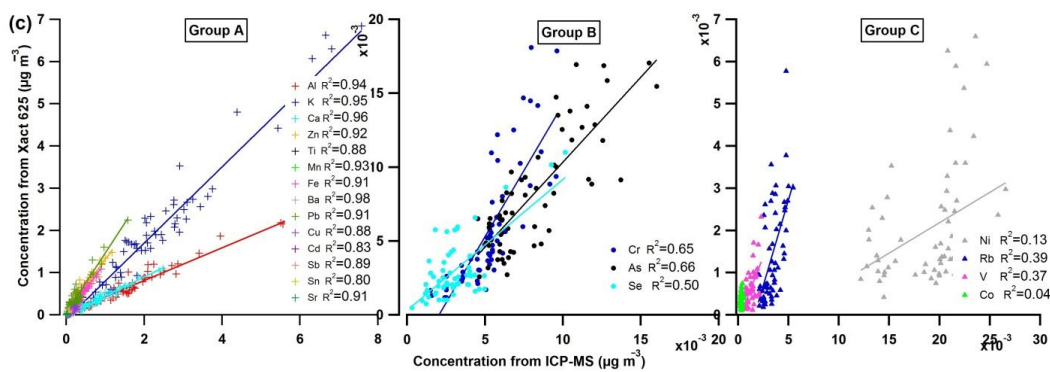
397

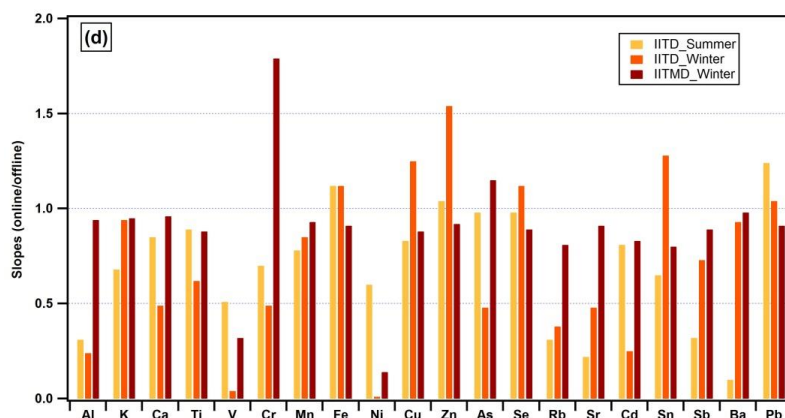


398



399





400

401 Fig. 6. Scatter plots and regression lines of Xact 625i vs. ICP-MS data for groups A, B, and C during (a)
402 summer at IITD, (b) winter at IITD, (c) winter at IITMD, and (d) comparison of slopes (online/offline) of
403 the measured heavy and trace metals in PM_{2.5} during the summer and winter campaign at IITD and
404 winter campaign at IITMD.

405 Based on their comparability characteristics, elements were grouped under 3 categories. Group A showed
406 excellent linearity between the two methods with a correlation coefficient of $R^2 > 0.8$. Overall, group A
407 consists of Al, K, Ca, Ti, Mn, Fe, Cu, Zn, Ba, and Pb during winter at IITD whereas, Cu showed in another
408 group during summer at IITD. Though Sr, Cd, Sn, Sb had average values below MDLs and posed a lower
409 correlation coefficient at IITD, interestingly, Sr, Cd, Sn, and Sb joined group A during winter at IITMD.
410 To distinguish the potential difference in accuracy between the two methods, intercepts were not forced to
411 be zero. The slopes are important, which indicate biases between the two measurements. The slopes of Zn,
412 Fe, and Pb were closer to unity during summer at IITD (Fig. 6). K, Fe, Cu, Zn, Ba, and Pb achieved a slope
413 of 0.94-1.25 during winter at IITD whereas, Mn, Fe, Zn, Pb, Sr, Sn, and Sb pose a slope slightly higher
414 than unity during winter at IITMD (Fig. 6). A slight difference in cut-off value for the particle size can
415 reduce the slopes from unity and produce ~10% difference in collected mass (Panteliadis et al., 2012). The
416 slopes and the correlation coefficients are listed in Table 3.

417 In a comparison study conducted by USEPA & Etv. (2012) between Xact 625i and ICP-MS measurements,
418 Ca, Cu, Mn, Pb, Se, and Zn were highly correlated except Cu. Cu was close to the MDL values of ICP-MS
419 and Xact 625i. A good agreement was observed between Xact 625i and offline measurements using ED-
420 XRF in South Korea by Park et al., (2014). The comparability between Xact measurements and ICP-MS
421 measurements was checked for the elements As, Ba, Ca, Cr, Cu, Fe, K, Mn, Ni, Pb, Se, Sr, Ti, V, and Zn



422 in Tremper et al. (2018). They observed an average R^2 of 0.93 and a slope of 1.07 for these elements. In the
 423 study by Furger et al., (2017) during a warmer season in Switzerland, an excellent correlation ($R^2 > 0.95$)
 424 was found for Xact and ICP-OES/MS measurements of S, K, Ca, Ti, Mn, Fe, Cu, Zn, Ba, and Pb. However,
 425 they found that the elemental measurements by Xact 625i were 28% higher than ICP-OES/MS
 426 measurements for these 10 elements. In our study, Xact measurements of Fe, Cu, Zn, and Pb yielded an
 427 average of 24% higher mass concentrations than ICP-MS measurements for Group A elements during
 428 winter at IITD. Xact measurements were systematically 10% (average) higher than ICP for Zn, Fe, and Pb
 429 during summer at IITD, whereas; we obtained an average of 41% higher Xact measurements than ICP for
 430 Mn, Fe, Zn, Pb, Sr, Sn, and Sb during winter at IITMD in Group A elements.

431 Group B was characterized by moderate linearity having $R^2 \sim 0.4-0.8$ and consisted of the elements V, Cu,
 432 As, and Se during summer at IITD; V, Cr, As, Se, Sn during winter at IITD and Cr, As and Se during winter
 433 at IITMD. These elements in Group B had their values very close to or below MDLs of at least one of the
 434 analysis methods. During winter at both sites, Cr and As from ICP-MS have ~50-65% of their values below
 435 MDLs, whereas ~68-72% of their values were above the MDLs of Xact 625i. Though some of the elements
 436 in this group in different seasons have slopes near or greater than unity (see Table 3) like Group A, their
 437 comparison is not statistically feasible.

438 Table 3. Regression coefficients and slopes for the comparison of Xact 625i and ICP-MS measurements.

Sites	Group A	Slope	R^2	Group B	Slope	R^2	Group C	Slope	R^2
IITD Summer	Al	0.31	0.81	V	0.51	0.59	Cr	0.7	0.29
	K	0.68	0.93	Cu	0.83	0.70	Co	-	-
	Ca	0.85	0.85	As	0.98	0.62	Rb	0.31	0.26
	Zn	1.04	0.83	Se	0.98	0.77	Sr	0.22	0.24
	Ba	0.1	0.94				Mo	-	-
	Ti	0.89	0.92				Cd	0.81	0.42
	Mn	0.78	0.92				Sn	0.65	0.41
	Fe	1.12	0.93				Sb	0.32	0.38
Pb	1.24	0.95				Ni	0.6	0.4	
IITD Winter	Al	0.24	0.89	V	0.04	0.48	Ni	0.01	0.07
	K	0.94	0.85	Cr	0.49	0.67	Rb	0.38	0.24
	Ca	0.49	0.89	As	0.48	0.42	Sr	0.48	0.34
	Ti	0.62	0.89	Se	1.12	0.75	Zr	-	-



IITD Winter	Mn	0.85	0.91	Sn	1.28	0.53	Cd	0.25	0.16
	Fe	1.12	0.81				Sb	0.73	0.40
	Cu	1.25	0.97						
	Zn	1.54	0.98						
	Ba	0.93	0.96						
	Pb	1.04	0.95						
	Al	0.94	0.39	Cr	1.79	0.65	Ni	0.14	0.13
	K	0.95	0.91	As	1.15	0.66	Rb	0.81	0.39
	Ca	0.96	0.45	Se	0.89	0.5	Mo	-	-
	Ti	0.88	0.72				Zr	-	-
	Mn	0.93	1.71				V	0.32	0.37
	Fe	0.91	1.29				Co	0.36	0.04
	Cu	0.88	0.70						
IITMD Winter	Zn	0.92	1.24						
	Ba	0.98	0.36						
	Pb	0.91	1.41						
	Sr	0.91	1.53						
	Cd	0.83	0.47						
	Sn	0.8	1.44						
	Sb	0.89	1.23						

439 The Group C elements, e.g., Ni, Rb, Sr, Zr, Cd, and Sb during summer at IITD; Cr, Co, Rb, Sr, Mo, Cd,
 440 Sn, Sb, and Ni during winter at IITD and, Ni, Rb, Mo, Zr, V, and Co during winter at IITMD are
 441 characterized by their bad correlation ($R^2 < 0.4$). Interestingly, measurements of some element e.g. Mo
 442 during summer and winter at IITD and IITMD respectively, Co during summer at IITD, and Zr during
 443 winter at both sites from both the methods did not correlate at all. For most of the elements in this group,
 444 70-85% of measurements were below both method's MDLs and rest of the data were below $3 \times$ MDLs.
 445 The high and variable blank concentrations of these elements increased the MDL values in ICP-MS
 446 measurement. The particle size dependent self-absorption effect and line interference between different
 447 elements in Xact measurement could also increase the MDL values (Furger et al., 2017). This is probably
 448 the reason for the values lower than MDLs for the elements in this group.

449 Overall, we observed 10-40% higher Xact measurements than ICP for some of the elements in Group A
 450 during different seasons. The difference in the Xact and High-volume sampler inlet location and their



451 distance from the road can cause such difference in measurements (Furger et al., 2017). In the case of dust
452 resuspension from vehicular traffic, the number concentration of finer particulate matter tends to decrease
453 sharply within an increment of just 50m from the roadway (Hagler et al., 2009). In this study, we tried to
454 co-locate the two sample inlets, but it could not be avoided. Also, IITD and IITMD are both very close
455 (<200 m) to a roadway with moderate to heavy-duty traffic. The differences in online and offline
456 measurements may indicate a gradient in some elements due to very close proximity to heavy-duty traffic.
457 Also, the different temperatures of the sample inlets may give rise to a difference in measured
458 concentrations from both methods (Tremper et al., 2018). In this study, the blank corrected ICP-MS
459 measurements may result in overestimation or underestimation due to variable and high blank
460 concentration. The difference can also occur due to the digestion recovery rate for the digestion protocol
461 used for the filter analysis. Moreover, if the ambient elemental concentration is much lower than the
462 standards used for calibration of Xact, such differences may occur (Indresand et al., 2013).

463 4. Conclusion

464 Atmospheric WSIS (NO_3^- , SO_4^{2-} , NH_4^+ , Cl^-) and heavy and trace elements in $\text{PM}_{2.5}$ were measured using
465 offline methods (IC for WSIS and ICP-MS for elements) and online methods (HR-ToF-AMS for inorganics
466 and Xact 625i for elements). These measurements were compared to assess the measurement quality and
467 sampling artifacts of these measurement techniques in the heavily polluted Delhi-NCR for two different
468 metrological conditions (winter and summer season). Field campaigns were conducted at two NCR sites,
469 namely, IITD during June-July 2019 and Oct-Dec 2019 and at IITMD during Oct-Dec 2019. The key
470 findings of this study are summarized below.

- 471 • NH_4^+ concentrations from the IC and HR-ToF-AMS, compared well during winter with a slope of
472 0.99 at IITD and 0.93 at IITMD. Interestingly, NH_4^+ concentrations were higher in offline
473 measurements during summer at IITD. The decrease in slope was probably due to the formation
474 of particulate $(\text{NH}_4)_2\text{SO}_4$.
- 475 • Offline SO_4^{2-} measurements were higher (with a slope of 0.17 during summer at IITD and 0.8 and
476 0.93 during winter at IITD and IITMD, respectively) during both seasons at both the sites due to
477 the positive sampling artifact. The absorption of SO_2 and the oxidation or condensation process
478 may result in additional sulphate.
- 479 • Lower NO_3^- concentrations (with a slope of 1.78 during summer at IITD and 1.07 during winter
480 at IITMD) were observed in the offline measurement during summer at IITD and during winter
481 at IITMD because of the evaporation of NH_4NO_3 from the filter substrates. The evaporative loss
482 of nitrate from the filters was minimal in winter at IITMD. It aggravated during summer at IITD



- 483 due to the evaporation of ammonium nitrate in such a high temperature (35°C-48°C) range. The
484 higher NO₃⁻ concentrations (slope~0.49) in the filters than HR-ToF-AMS measurements during
485 winter at IITD can be due to the absorption of gas-phase HNO₃ on the filter.
- 486 • Offline Cl⁻ was consistently higher (with a slope of 0.33 during summer at IITD and 0.79 and 0.88
487 during winter at IITD and IITMD, respectively) than HR-ToF-AMS measurements during both
488 seasons at both sites mainly because HR-ToF-AMS only measures the NR-Cl⁻ whereas, the offline
489 Cl⁻ measurements includes chloride from all the water-soluble chloride salts. The comparability
490 degrades during summer due to the volatile nature of Cl⁻ in higher temperatures and lower RH.
 - 491 • The elements were grouped into three categories (Group A, B and C) according to their
492 comparability characteristics. The elemental data from Xact 625i were highly correlated (R²>0.8)
493 with ICP-MS measurements of the 24 hr filters for Group A elements (Al, K, Ca, Ti, Zn, Mn, Fe,
494 Ba, and Pb). The Cu also showed up in this group during winter at IITD. About 80% of the data
495 for these elements were above MDLs for both the methods. Though Sn, Sb, and Cd had values
496 below MDLs of one or both the methods, interestingly, they were highly correlated (R²>0.8) and,
497 slopes are very close to unity for Sn and Sb during winter at IITMD. The correlation coefficients
498 > 0.8 for the elements in Group A indicated the high precision of the online and offline
499 measurements. Hence, these elements from any of these methods can be reliably used for
500 modelling studies.
 - 501 • The elements under Group B had their values closer to or below at least one of the method's
502 MDLs. Cr and As had ~50-65% of their values below ICP-MS MDLs from ICP-MS, whereas
503 ~68-72% of their values were above Xact 625i MDLs during winter at both sites.
 - 504 • Elements like Ni, Mo, and Zr measured from ICP-MS were not reliable due to their higher and
505 variable blank concentrations. No conclusion on their measurement accuracy by the two methods
506 can be drawn.
 - 507 • In summary, the daily averaged half-hourly Xact 625i measurements were 10-40% higher than 24
508 hr filter measurements by ICP-MS depending upon the seasons, sites and elements in Group A.
509 Distance between two inlets for the two methods, distance of the inlets from the roadway, line
510 interference between two elements in Xact measurements, particle size, sampling strategy, filter
511 type, higher and variable concentrations in blank filters and digestion protocol for ICP
512 measurements can cause the difference in measurements between the two methods.

513 The above findings highlight the measurement methods' accuracy and implement the particular type of
514 measurements as needed. Future work should involve using different filter substrates and different
515 digestion protocols to reevaluate the difference between these online and offline methods. Although this



516 study compares the PM species, a comparison of full source apportionment analysis between online and
517 offline methods should be done for more qualitative and quantitative insights.

518 **Author contribution**

519 HSB performed the offline analysis, data processing and wrote the manuscript. JD collected the AMS data
520 at IITD. AS and VL carried out the Xact and AMS data collection and processing respectively. NR, MK,
521 VS and SNT were involved with the supervision and conceptualization. All co-authors contributed to the
522 paper discussion and revision.

523 **Declaration of interests**

524 The authors declare that they have no conflict of interest.

525 **Acknowledgements**

526 The authors are thankful to Naba Hazarika and Mohd Faisal for collecting the Xact data at IITMD and
527 Pawan Vats for the sampling and collection of the filters at IITD. The authors are also thankful to Amit
528 Vishwakarma, Vaibhav Shrivastava and Harishankar for helping in offline analysis. This work is financially
529 supported by the Department of Biotechnology, Government of India (Grant No.
530 BT/IN/UK/APHH/41/KB/2016-17 dated 19th July 2017) and Central Pollution Control Board (CPCB),
531 Government of India to conduct this research under grant no. AQM/Source apportionment_EPC
532 Project/2017 dated 12th February 2019.

533 **Reference**

534 Bhowmik, H. S., Naresh, S., Bhattu, D., Rastogi, N., Prévôt, A. S. H., & Tripathi, S. N. (2020). Temporal and spatial
535 variability of carbonaceous species (EC; OC; WSOC and SOA) in PM_{2.5} aerosol over five sites of Indo-
536 Gangetic Plain. *Atmospheric Pollution Research*, 12(June 2020), 375–390.
537 <https://doi.org/10.1016/j.apr.2020.09.019>

538 Canagaratna, M.R., Jayne, J.T., Jimenez, J.L., Allan, J.D., Alfarra, M.R., Zhang, Q., Onasch, T.B., Drewnick, F.,
539 Coe, H., Middlebrook, A., Delia, A., Williams, L.R., Trimborn, A.M., Northway, M.J., DeCarlo, P.F., Kolb,
540 C.E., Davidovits, P., Worsnop, D.R., 2007. Chemical and microphysical characterization of ambient aerosols
541 with the aerodyne aerosol mass spectrometer. *Mass Spectrom. Rev.* <https://doi.org/10.1002/mas.20115>.

542 CEN: *Ambient air – Standard gravimetric measurement method for the determination of the PM₁₀ or PM_{2.5} mass*
543 *concentration of suspended particulate matter* (EN 12341:2014), European Committee for Standardization (CEN),
544 Brussels. 2014.



- 545
546 Chow, J. C. (1995). Measurement methods to determine compliance with ambient air quality standards for
547 suspended particles. *Journal of the Air and Waste Management Association*, 45(5), 320–382.
548 <https://doi.org/10.1080/10473289.1995.10467369>
- 549 Chow, J. C., Watson, J. G., Lowenthal, D. H., Park, K., Doraiswamy, P., Bowers, K., & Bode, R. (2008).
550 Continuous and filter-based measurements of PM_{2.5} nitrate and sulfate at the Fresno Supersite. *Environmental*
551 *Monitoring and Assessment*, 144(1–3), 179–189. <https://doi.org/10.1007/s10661-007-9987-5>
- 552 DeCarlo, P. F., Kimmel, J. R., Trimborn, A., Northway, M. J., Jayne, J. T., Aiken, A. C., Gonin, M., Fuhrer, K.,
553 Horvath, T., Docherty, K. S., Worsnop, D. R., & Jimenez, J. L. (2006). Field-deployable, high-resolution,
554 time-of-flight aerosol mass spectrometer. *Analytical Chemistry*, 78(24), 8281–8289.
555 <https://doi.org/10.1021/ac061249n>
- 556 Escrig Vidal, A., Monfort, E., Celades, I., Querol, X., Amato, F., Minguillón, M. C., & Hopke, P. K. (2009).
557 Application of optimally scaled target factor analysis for assessing source contribution of ambient PM₁₀.
558 *Journal of the Air and Waste Management Association*, 59(11), 1296–1307. [https://doi.org/10.3155/1047-](https://doi.org/10.3155/1047-3289.59.11.1296)
559 [3289.59.11.1296](https://doi.org/10.3155/1047-3289.59.11.1296)
- 560 Furger, M., Minguillón, M. C., Yadav, V., Slowik, J. G., Hüglin, C., Fröhlich, R., Petterson, K., Baltensperger, U.,
561 & Prévôt, A. S. H. (2017). Elemental composition of ambient aerosols measured with high temporal resolution
562 using an online XRF spectrometer. *Atmospheric Measurement Techniques*, 10(6), 2061–2076.
563 <https://doi.org/10.5194/amt-10-2061-2017>
- 564 Gani, S., Bhandari, S., Seraj, S., Wang, D. S., Patel, K., Soni, P., Arub, Z., Habib, G., Hildebrandt Ruiz, L., & Apte,
565 J. S. (2019). Submicron aerosol composition in the world's most polluted megacity: The Delhi Aerosol
566 Supersite study. *Atmospheric Chemistry and Physics*, 19(10), 6843–6859. [https://doi.org/10.5194/acp-19-](https://doi.org/10.5194/acp-19-6843-2019)
567 [6843-2019](https://doi.org/10.5194/acp-19-6843-2019)
- 568 Hagler, G. S. W., Baldauf, R. W., Thoma, E. D., Long, T. R., Snow, R. F., Kinsey, J. S., Oudejans, L., & Gullett, B.
569 K. (2009). Ultrafine particles near a major roadway in Raleigh, North Carolina: Downwind attenuation and
570 correlation with traffic-related pollutants. *Atmospheric Environment*, 43(6), 1229–1234.
571 <https://doi.org/10.1016/j.atmosenv.2008.11.024>
- 572 Hong, C., Zhang, Q., Zhang, Y., Davis, S. J., Tong, D., Zheng, Y., Liu, Z., Guan, D., He, K., & Schellnhuber, H. J.
573 (2019). Impacts of climate change on future air quality and human health in China. *Proceedings of the*
574 *National Academy of Sciences of the United States of America*, 116(35), 17193–17200.
575 <https://doi.org/10.1073/pnas.1812881116>
- 576 Indresand, H., White, W. H., Trzepla, K., & Dillner, A. M. (2013). Preparation of sulfur reference materials that
577 reproduce atmospheric particulate matter sample characteristics for XRF calibration. *X-Ray Spectrometry*,



- 578 42(5), 359–367. <https://doi.org/10.1002/xrs.2456>
- 579 Jayne, J. T., Leard, D. C., Zhang, X., Davidovits, P., Smith, K. A., Kolb, C. E., & Worsnop, D. R. (2000).
580 Development of an aerosol mass spectrometer for size and composition analysis of submicron particles. In
581 *Aerosol Science and Technology* (Vol. 33, Issues 1–2, pp. 49–70). <https://doi.org/10.1080/027868200410840>
- 582 Jimenez, J. L., Jayne, J. T., Shi, Q., Kolb, C. E., Worsnop, D. R., Yourshaw, I., Seinfeld, J. H., Flagan, R. C., Zhang,
583 X., Smith, K. A., Morris, J. W., & Davidovits, P. (2003). Ambient aerosol sampling using the Aerodyne
584 aerosol mass spectrometer. *Journal of Geophysical Research: Atmospheres*, 108(7).
585 <https://doi.org/10.1029/2001jd001213>
- 586 Lalchandani, V., Kumar, V., Tobler, A., M. Thamban, N., Mishra, S., Slowik, J. G., Bhattu, D., Rai, P., Satish, R.,
587 Ganguly, D., Tiwari, S., Rastogi, N., Tiwari, S., Močnik, G., Prévôt, A. S. H., & Tripathi, S. N. (2021). Real-
588 time characterization and source apportionment of fine particulate matter in the Delhi megacity area during
589 late winter. *Science of the Total Environment*, 770. <https://doi.org/10.1016/j.scitotenv.2021.145324>
- 590 Lipfert, F. W. (1994). Filter artifacts associated with particulate measurements: Recent evidence and effects on
591 statistical relationships. *Atmospheric Environment*, 28(20), 3233–3249. [https://doi.org/10.1016/1352-](https://doi.org/10.1016/1352-2310(94)00167-J)
592 [2310\(94\)00167-J](https://doi.org/10.1016/1352-2310(94)00167-J)
- 593 Makkonen, U., Virkkula, A., Mäntykenttä, J., Hakola, H., Keronen, P., Vakkari, V., & Aalto, P. P. (2012). Semi-
594 continuous gas and inorganic aerosol measurements at a Finnish urban site: Comparisons with filters, nitrogen
595 in aerosol and gas phases, and aerosol acidity. *Atmospheric Chemistry and Physics*, 12(12), 5617–5631.
596 <https://doi.org/10.5194/acp-12-5617-2012>
- 597 Malaguti, A., Mircea, M., La Torretta, T. M. G., Telloli, C., Petralia, E., Stracquadiano, M., & Berico, M. (2015).
598 Comparison of online and offline methods for measuring fine secondary inorganic ions and carbonaceous
599 aerosols in the central mediterranean area. *Aerosol and Air Quality Research*, 15(7), 2641–2653.
600 <https://doi.org/10.4209/aaqr.2015.04.0240>
- 601 Manchanda, C., Kumar, M., Singh, V., Faisal, M., Hazarika, N., Shukla, A., Lalchandani, V., Goel, V., Thamban,
602 N., Ganguly, D., & Tripathi, S. N. (2021). Variation in chemical composition and sources of PM_{2.5} during the
603 COVID-19 lockdown in Delhi. *Environment International*, 153(December 2020), 106541.
604 <https://doi.org/10.1016/j.envint.2021.106541>
- 605 Minguillón, M. C., Querol, X., Baltensperger, U., & Prévôt, A. S. H. (2012). Fine and coarse PM composition and
606 sources in rural and urban sites in Switzerland: Local or regional pollution? *Science of the Total Environment*,
607 427–428, 191–202. <https://doi.org/10.1016/j.scitotenv.2012.04.030>
- 608 Nagar, P. K., Singh, D., Sharma, M., Kumar, A., Aneja, V. P., George, M. P., Agarwal, N., & Shukla, S. P. (2017).
609 Characterization of PM_{2.5} in Delhi: role and impact of secondary aerosol, burning of biomass, and municipal



- 610 solid waste and crustal matter. *Environmental Science and Pollution Research*, 24(32), 25179–25189.
611 <https://doi.org/10.1007/s11356-017-0171-3>
- 612 Nicolás, J. F., Galindo, N., Yubero, E., Pastor, C., Esclapez, R., & Crespo, J. (2009). Aerosol inorganic ions in a
613 semiarid region on the Southeastern Spanish mediterranean coast. *Water, Air, and Soil Pollution*, 201(1–4),
614 149–159. <https://doi.org/10.1007/s11270-008-9934-2>
- 615 Nie, W., Wang, T., Gao, X., Pathak, R. K., Wang, X., Gao, R., Zhang, Q., Yang, L., & Wang, W. (2010).
616 Comparison among filter-based, impactor-based and continuous techniques for measuring atmospheric fine
617 sulfate and nitrate. *Atmospheric Environment*, 44(35), 4396–4403.
618 <https://doi.org/10.1016/j.atmosenv.2010.07.047>
- 619 Pakkanen, T. A., & Hillamo, R. E. (2002). Comparison of sampling artifacts and ion balances for a Berner low-
620 pressure impactor and a virtual impactor. *Boreal Environment Research*, 7(2), 129–140.
- 621 Pandolfi, M., Querol, X., Alastuey, A., Jimenez, J. L., Jorba, O., Day, D., Ortega, A., Cubison, M. J., Comerón, A.,
622 Sicard, M., Mohr, C., Prévôt, A. S. H., Minguillón, M. C., Pey, J., Baldasano, J. M., Burkhardt, J. F., Seco, R.,
623 Peñuelas, J., Van Drooge, B. L., ... Szidat, S. (2014). Effects of sources and meteorology on particulate matter
624 in the Western Mediterranean Basin: An overview of the DAURE campaign. *Journal of Geophysical*
625 *Research*, 119(8), 4978–5010. <https://doi.org/10.1002/2013JD021079>
- 626 Pant, P., Shukla, A., Kohl, S. D., Chow, J. C., Watson, J. G., & Harrison, R. M. (2015). Characterization of ambient
627 PM_{2.5} at a pollution hotspot in New Delhi, India and inference of sources. *Atmospheric Environment*, 109,
628 178–189. <https://doi.org/10.1016/j.atmosenv.2015.02.074>
- 629 Panteliadis, P., Helmink, H. J. P., Koopman, P. C., Hoonhout, M., Jonge, D. De, & Visser, J. H. (2012). *PM 10*
630 *sampling inlets comparison : EPA vs EU. 12341(1999)*, 12341.
- 631 Park, S. S., Cho, S. Y., Jo, M. R., Gong, B. J., Park, J. S., & Lee, S. J. (2014). Field evaluation of a near-real time
632 elemental monitor and identification of element sources observed at an air monitoring supersite in Korea.
633 *Atmospheric Pollution Research*, 5(1), 119–128. <https://doi.org/10.5094/APR.2014.015>
- 634 Patel, A., Rastogi, N., Gandhi, U., & Khatri, N. (2021). Oxidative potential of atmospheric PM₁₀ at five different
635 sites of Ahmedabad, a big city in Western India. *Environmental Pollution*, 268, 115909.
636 <https://doi.org/10.1016/j.envpol.2020.115909>
- 637 Pathak, R. K., & Chan, C. K. (2005). Inter-particle and gas-particle interactions in sampling artifacts of PM_{2.5} in
638 filter-based samplers. *Atmospheric Environment*, 39(9), 1597–1607.
639 <https://doi.org/10.1016/j.atmosenv.2004.10.018>
- 640 Peck, J., Gonzalez, L. A., Williams, L. R., Xu, W., Croteau, P. L., Timko, M. T., Jayne, J. T., Worsnop, D. R.,
641 Miake-Lye, R. C., & Smith, K. A. (2016). Development of an aerosol mass spectrometer lens system for



- 642 PM2.5. *Aerosol Science and Technology*, 50(8), 781–789. <https://doi.org/10.1080/02786826.2016.1190444>
- 643 Pope, C. A., Ezzati, M., & Dockery, D. W. (2009). Fine-Particulate Air Pollution and Life Expectancy in the United
644 States. *New England Journal of Medicine*, 360(4), 376–386. <https://doi.org/10.1056/nejmsa0805646>
- 645 Querol, X., Pey, J., Minguillón, M. C., Pérez, N., Alastuey, A., Viana, M., Moreno, T., Bernabé, R. M., Blanco, S.,
646 Cárdenas, B., Vega, E., Sosa, G., Escalona, S., Ruiz, H., & Artíñano, B. (2008). PM speciation and sources in
647 Mexico during the MILAGRO-2006 campaign. *Atmospheric Chemistry and Physics*, 8(1), 111–128.
648 <https://doi.org/10.5194/acp-8-111-2008>
- 649 Rai, P., Furger, M., El Haddad, I., Kumar, V., Wang, L., Singh, A., Dixit, K., Bhattu, D., Petit, J. E., Ganguly, D.,
650 Rastogi, N., Baltensperger, U., Tripathi, S. N., Slowik, J. G., & Prévôt, A. S. H. (2020). Real-time
651 measurement and source apportionment of elements in Delhi's atmosphere. *Science of the Total Environment*,
652 742. <https://doi.org/10.1016/j.scitotenv.2020.140332>
- 653 Rai, P., Slowik, J. G., Furger, M., El Haddad, I., Visser, S., Tong, Y., Singh, A., Wehrle, G., Kumar, V., Tobler, A.
654 K., Bhattu, D., Wang, L., Ganguly, D., Rastogi, N., Huang, R. J., Necki, J., Cao, J., Tripathi, S. N.,
655 Baltensperger, U., & Prevot, A. S. H. (2021). Highly time-resolved measurements of element concentrations
656 in PM10 and PM2.5: Comparison of Delhi, Beijing, London, and Krakow. *Atmospheric Chemistry and
657 Physics*, 21(2), 717–730. <https://doi.org/10.5194/acp-21-717-2021>
- 658 Rastogi, N., & Sarin, M. M. (2005). Long-term characterization of ionic species in aerosols from urban and high-
659 altitude sites in western India: Role of mineral dust and anthropogenic sources. *Atmospheric Environment*,
660 39(30), 5541–5554. <https://doi.org/10.1016/j.atmosenv.2005.06.011>
- 661 Rengarajan, R., Sarin, M. M., & Sudheer, A. K. (2007). Carbonaceous and inorganic species in atmospheric aerosols
662 during wintertime over urban and high-altitude sites in North India. *Journal of Geophysical Research
663 Atmospheres*, 112(21), 1–16. <https://doi.org/10.1029/2006JD008150>
- 664 Schaap, M., Spindler, G., Schulz, M., Acker, K., Maenhaut, W., Berner, A., Wieprecht, W., Streit, N., Müller, K.,
665 Brüggemann, E., Chi, X., Putaud, J. P., Hitzenberger, R., Puxbaum, H., Baltensperger, U., & Ten Brink, H.
666 (2004). Artefacts in the sampling of nitrate studied in the “iINTERCOMP” campaigns of EUROTRAC-
667 AEROSOL. *Atmospheric Environment*, 38(38), 6487–6496. <https://doi.org/10.1016/j.atmosenv.2004.08.026>
- 668 Sharma, D., & Kulshrestha, U. C. (2014). Spatial and temporal patterns of air pollutants in rural and urban areas of
669 India. *Environmental Pollution*, 195(2), 276–281. <https://doi.org/10.1016/j.envpol.2014.08.026>
- 670 Sharma, S. K., Mandal, T. K., Jain, S., Saraswati, Sharma, A., & Saxena, M. (2016). Source Apportionment of
671 PM2.5 in Delhi, India Using PMF Model. *Bulletin of Environmental Contamination and Toxicology*, 97(2),
672 286–293. <https://doi.org/10.1007/s00128-016-1836-1>
- 673 Shukla, A. K., Lalchandani, V., Bhattu, D., Dave, J. S., Rai, P., Thamban, N. M., Mishra, S., Gaddamidi, S.,



- 674 Tripathi, N., Vats, P., Rastogi, N., Sahu, L., Ganguly, D., Kumar, M., Singh, V., Gargava, P., & Tripathi, S. N.
675 (2021). Real-time quantification and source apportionment of fine particulate matter including organics and
676 elements in Delhi during summertime. *Atmospheric Environment*, 261(July), 118598.
677 <https://doi.org/10.1016/j.atmosenv.2021.118598>
- 678 Singh, A., Rastogi, N., Kumar, V., Slowik, J. G., Satish, R., Lalchandani, V., Thamban, N. M., Rai, P., Bhattu, D.,
679 Vats, P., Ganguly, D., Tripathi, S. N., & Prévôt, A. S. H. (2021). Sources and characteristics of light-absorbing
680 fine particulates over Delhi through the synergy of real-time optical and chemical measurements. *Atmospheric
681 Environment*, 252(March). <https://doi.org/10.1016/j.atmosenv.2021.118338>
- 682 Singh, A., Satish, R. V., & Rastogi, N. (2019). Characteristics and sources of fine organic aerosol over a big semi-
683 arid urban city of western India using HR-ToF-AMS. *Atmospheric Environment*, 208(April), 103–112.
684 <https://doi.org/10.1016/j.atmosenv.2019.04.009>
- 685 Singhai, A., Habib, G., Raman, R. S., & Gupta, T. (2017). Chemical characterization of PM1.0 aerosol in Delhi and
686 source apportionment using positive matrix factorization. *Environmental Science and Pollution Research*,
687 24(1), 445–462. <https://doi.org/10.1007/s11356-016-7708-8>
- 688 Takahama, S., Wittig, A. E., Vayenas, D. V., Davidson, C. I., & Pandis, S. N. (2004). Modeling the diurnal variation
689 of nitrate during the Pittsburgh Air Quality Study. *Journal of Geophysical Research D: Atmospheres*, 109(16).
690 <https://doi.org/10.1029/2003JD004149>
- 691 Tobler, A., Bhattu, D., Canonaco, F., Lalchandani, V., Shukla, A., Thamban, N. M., Mishra, S., Srivastava, A. K.,
692 Bisht, D. S., Tiwari, S., Singh, S., Močnik, G., Baltensperger, U., Tripathi, S. N., Slowik, J. G., & Prévôt, A.
693 S. H. (2020). Chemical characterization of PM2.5 and source apportionment of organic aerosol in New Delhi,
694 India. *Science of the Total Environment*, 745. <https://doi.org/10.1016/j.scitotenv.2020.140924>
- 695 Tremper, A. H., Font, A., Priestman, M., Hamad, S. H., Chung, T. C., Pribadi, A., Brown, R. J. C., Goddard, S. L.,
696 Grassineau, N., Petterson, K., Kelly, F. J., & Green, D. C. (2018). Field and laboratory evaluation of a high
697 time resolution x-ray fluorescence instrument for determining the elemental composition of ambient aerosols.
698 *Atmospheric Measurement Techniques*, 11(6), 3541–3557. <https://doi.org/10.5194/amt-11-3541-2018>
- 699 US-EPA: *Determination of metals in ambient particulate matter using X-Ray Fluorescence (XRF) Spectroscopy*,
700 Agency, edited by: US-EPA (US Environmental Protection Agency), Cincinnati, OH 45268, USA, 1999.
701
- 702 Usepa, & Etv. (2012). *Environmental Technology Verification Report Cooper Environmental Services LLC † Xact
703 625 Particulate Metals Monitor. September 2012.* <http://cooperenvironmental.com/>
- 704 Viana, M., Chi, X., Maenhaut, W., Cafmeyer, J., Querol, X., Alastuey, A., Mikuška, P., & Večeřa, Z. (2006).
705 Influence of sampling artefacts on measured PM, OC, and EC levels in carbonaceous aerosols in an urban
706 area. *Aerosol Science and Technology*, 40(2), 107–117. <https://doi.org/10.1080/02786820500484388>



- 707 Wang, M., Aaron, C. P., Madrigano, J., Hoffman, E. A., Angelini, E., Yang, J., Laine, A., Vetterli, T. M., Kinney, P.
708 L., Sampson, P. D., Sheppard, L. E., Szpiro, A. A., Adar, S. D., Kirwa, K., Smith, B., Lederer, D. J., Diez-
709 Roux, A. V., Vedal, S., Kaufman, J. D., & Barr, R. G. (2019). Association between long-term exposure to
710 ambient air pollution and change in quantitatively assessed emphysema and lung function. *JAMA - Journal of*
711 *the American Medical Association*, 322(6), 546–556. <https://doi.org/10.1001/jama.2019.10255>
- 712 World Health Organisation, 2018. WHO Global Ambient Air Quality Database (Update 2018) [WWW Document].
713 Ambient Air Qual. Database (Update 2018).
714
- 715 Wu, W. S., & Wang, T. (2007). On the performance of a semi-continuous PM_{2.5} sulphate and nitrate instrument
716 under high loadings of particulate and sulphur dioxide. *Atmospheric Environment*, 41(26), 5442–5451.
717 <https://doi.org/10.1016/j.atmosenv.2007.02.025>
- 718 Yardley, R. E., Sweeney, B. P., Butterfield, D., Quincey, P., and Fuller, G. W.: *Estimation of Measurement*
719 *Uncertainty in Network Data*, National Physical Laboratory, 13–36, 2007.
- 720 Zhang, D., Shi, G. Y., Iwasaka, Y., & Hu, M. (2000). Mixture of sulfate and nitrate in coastal atmospheric aerosols:
721 Individual particle studies in Qingdao (36°04'N, 120°21'E), China. *Atmospheric Environment*, 34(17), 2669–
722 2679. [https://doi.org/10.1016/S1352-2310\(00\)00078-9](https://doi.org/10.1016/S1352-2310(00)00078-9)
- 723 Zhang, X., & McMurry, P. H. (1992). EVAPORATIVE LOSSES OF FINE PARTICULATE NITRATES DURING
724 SAMPLING. In *Atmospheric Environment* (Vol. 26, Issue 18).
- 725